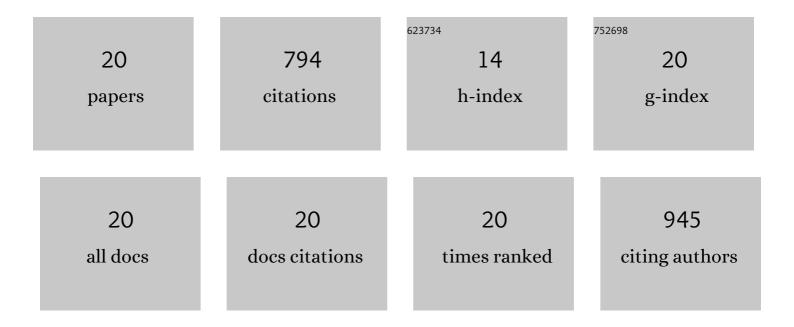
S M Hansen

List of Publications by Year in descending order

Source: https://exaly.com/author-pdf/8080686/publications.pdf Version: 2024-02-01



S M HANSEN

#	Article	lF	CITATIONS
1	Seismic Evidence of Bottomâ€Up Crustal Control on Volcanism and Magma Storage Near Mount St. Helens. Geophysical Research Letters, 2021, 48, e2020GL090612.	4.0	2
2	Local Source <i>Vp</i> and <i>Vs</i> Tomography in the Mount St. Helens Region With the iMUSH Broadband Array. Geochemistry, Geophysics, Geosystems, 2020, 21, e2019GC008888.	2.5	26
3	Seismic evidence for a fossil slab origin for the Isabella anomaly. Geophysical Journal International, 2020, 224, 1188-1196.	2.4	6
4	Multiscale imaging of the Earth's interior with Receiver Function Scattering Kernels. Acta Geologica Sinica, 2019, 93, 329-329.	1.4	2
5	Upper Crustal Structure and Magmatism in Southwest Washington: <i>V</i> _{<i>p</i>} , <i>V</i> _{<i>s</i>} , and <i>V</i> _{<i>p</i>} / <i>V</i> _{<i>s</i>} Results From the iMUSH Activeâ€Source Seismic Experiment. Journal of Geophysical Research: Solid Earth, 2019, 124. 7067-7080.	3.4	5
6	Rayleigh and S wave tomography constraints on subduction termination and lithospheric foundering in central California. Earth and Planetary Science Letters, 2018, 488, 14-26.	4.4	35
7	Focusing of melt near the top of the Mount St. Helens (USA) magma reservoir and its relationship to major volcanic eruptions. Geology, 2018, 46, 775-778.	4.4	36
8	Upper crustal low-frequency seismicity at Mount St. Helens detected with a dense geophone array. Journal of Volcanology and Geothermal Research, 2018, 358, 329-341.	2.1	16
9	Seismic array constraints on reach-scale bedload transport. Geology, 2017, 45, 299-302.	4.4	36
10	<i>P</i> and <i>S</i> Wave Receiver Function Imaging of Subduction With Scattering Kernels. Geochemistry, Geophysics, Geosystems, 2017, 18, 4487-4502.	2.5	24
11	Magma reservoirs from the upper crust to the Moho inferred from high-resolution Vp and Vs models beneath Mount St. Helens, Washington State, USA. Geology, 2016, 44, 411-414.	4.4	94
12	Seismic evidence for a cold serpentinized mantle wedge beneath Mount St Helens. Nature Communications, 2016, 7, 13242.	12.8	42
13	Automated detection and location of microseismicity at Mount St. Helens with a largeâ€N geophone array. Geophysical Research Letters, 2015, 42, 7390-7397.	4.0	70
14	Thermal classification of lithospheric discontinuities beneath USArray. Earth and Planetary Science Letters, 2015, 431, 36-47.	4.4	80
15	Seismic tomography of the Colorado Rocky Mountains upper mantle from CREST: Lithosphere–asthenosphere interactions and mantle support of topography. Earth and Planetary Science Letters, 2014, 402, 107-119.	4.4	13
16	A rootless rockies—Support and lithospheric structure of the Colorado Rocky Mountains inferred from CREST and TA seismic data. Geochemistry, Geophysics, Geosystems, 2013, 14, 2670-2695.	2.5	65
17	Hot mantle upwelling across the 660 beneath Yellowstone. Earth and Planetary Science Letters, 2012, 331-332, 224-236.	4.4	112
18	A sporadic low-velocity layer atop the western U.S. mantle transition zone and short-wavelength variations in transition zone discontinuities. Geochemistry, Geophysics, Geosystems, 2011, 12, n/a-n/a.	2.5	40

#	Article	IF	CITATIONS
19	Characterizing the 410 km discontinuity lowâ€velocity layer beneath the LA RISTRA array in the North American Southwest. Geochemistry, Geophysics, Geosystems, 2010, 11, .	2.5	42
20	P- and S-Wave Receiver Function Images of Crustal Imbrication beneath the Cheyenne Belt in Southeast Wyoming. Bulletin of the Seismological Society of America, 2009, 99, 1953-1961.	2.3	48